# Correlating fragility and heterogeneous dynamics in polystyrene through single molecule studies

Cite as: J. Chem. Phys. 151, 084501 (2019); doi: 10.1063/1.5114905

Submitted: 12 June 2019 · Accepted: 31 July 2019 ·

Published Online: 22 August 2019







Alyssa S. Manz, D Mariam Aly, and Laura J. Kaufman D



Department of Chemistry, Columbia University, New York, New York 10027, USA

a) Author to whom correspondence should be addressed: kaufman@chem.columbia.edu

#### **ABSTRACT**

Many macroscopic properties of polymers depend on their molecular weight, with one notable example being glass transition temperature: polymers with higher molecular weights typically have higher glass transition temperatures than their lower molecular weight polymeric and oligomeric counterparts. Polymeric systems close to their glass transition temperatures also exhibit interesting properties, showing both high (and molecular weight dependent) fragility and strong evidence of dynamic heterogeneity. While studies have detailed the correlations between molecular weight and fragility, studies clearly detailing correlations between molecular weight and degree of heterogeneous dynamics are lacking. In this study, we use single molecule rotational measurements to investigate the impact of molecular weight on polystyrene's degree of heterogeneity near its glass transition temperature. To this end, two types of fluorescent probes are embedded in films composed of polystyrene ranging from 0.6 to 1364.0 kg mol<sup>-1</sup>. We find correlation between polystyrene molecular weight, fragility, and degree of dynamic heterogeneity as reported by single molecule stretching exponents but do not find clear correlation between these quantities and time scales associated with dynamic exchange.

Published under license by AIP Publishing. https://doi.org/10.1063/1.5114905

#### INTRODUCTION

It is well known that the chain length, and thus molecular weight, of polymers influences many of their macroscopic characteristics. In fact, Fox and Flory reported on molecular weight dependent properties including the viscoelastic behavior and glass transition temperature (Tg) of polystyrene as early as the mid-20th century.<sup>1-4</sup> A multitude of additional studies on the influence of molecular weight on polymers in the rubbery regime—i.e., between their melting point and glass transition temperature—have followed. For polystyrene, in particular, it has been noted that fragility increases as molecular weight increases, at least in some molecular weight regimes. 5-7 Fragility, m, is a parameter that describes the degree to which the temperature dependence of the viscosity or structural relaxation time near the glass transition temperature of a system is non-Arrhenius.8 Fragility is thus a well-accepted measure of anomalous behavior in glass-forming systems, with high fragility being a mark of highly anomalous behavior. 9-11

Empirical correlations between fragility and other quantities that characterize anomalous behavior in glassy systems have been identified, with one such quantity being the stretching exponent. 12,13

Stretching exponents characterize the degree to which fluctuations and relaxations present in glass formers near the glass transition temperature are nonexponential. These complex fluctuations and relaxations are typically characterized with the Kohlrausch-Williams-Watts (KWW) equation  $[C(t) = C(0)^* \exp[-(t/\tau_{fit})^{\beta}]$ , with β being the stretching exponent, whose deviation below 1 signifies divergence from the exponential decay associated with liquids far above Tg. Nonexponential behaviors in glassy materials have been associated with dynamic heterogeneity, in which dynamics vary as a function of both position (spatial heterogeneity) and time (temporal heterogeneity), even in the absence of identifiable structural heterogeneity. 14-16 The reported anticorrelation between fragility and stretching exponent undergirds the idea that both quantities encode information about dynamic heterogeneity and the related issue of degree of cooperative dynamics in glassy systems. 12,13,17,18

Recently, we used single molecule measurements to study polystyrene of a given molecular weight (168 kg mol<sup>-1</sup>), showing that neither stretching exponent nor time scales associated with temporal heterogeneity vary over temperature from 1.00 to 1.02 Tg. 15 Here, we use a similar approach to characterize polystyrene over a range of molecular weights (0.6–1364.0 kg mol $^{-1}$ ) that alter its fragility from m  $\approx 75$ –120 while simultaneously shifting its glass transition temperature by more than 100 K. These experiments clarify whether the (1) reported correlations between fragility and stretching exponent hold when stretching exponents are obtained from single molecule measurements and (2) time scales of dynamic exchange, which have also been associated with the degree of dynamic heterogeneity, vary as a function of polystyrene molecular weight.  $^{20-23}$ 

#### **MATERIALS AND METHODS**

# Sample preparation

Polystyrene samples of 0.6 kg mol<sup>-1</sup> (PDI = 1.05), 6.4 kg mol<sup>-1</sup> (PDI = 1.2), 27.5 kg mol<sup>-1</sup> (PDI = 1.3), 168.0 kg mol<sup>-1</sup> (PDI = 1.05), and 1364.0 kg mol<sup>-1</sup> (PDI = 1.3) were obtained from Polymer Source. All samples except the lowest molecular weight polystyrene were reprecipitated in hexane a minimum of two times and then dissolved in toluene to yield solutions of 8.0 wt. % (6.4 kg mol<sup>-1</sup>), 6.8 wt. % (27.5 kg mol<sup>-1</sup>), 3.4 wt. % (168.0 kg mol<sup>-1</sup>), and 3.1 wt. % (1364 kg mol<sup>-1</sup>) polystyrene. These solutions were then photobleached in a home-built light emitting diode (LED) based setup at 533 nm for at least 48 h to achieve a nonfluorescent host. Due to its comparatively low glass transition temperature, the 0.6 kg mol<sup>-1</sup> polystyrene sample was not reprecipitated in hexane, but rather dissolved in toluene, resulting in a 10.0 wt. % solution, which was photobleached for a minimum of one week.

Two fluorescent dyes were used in this study. The dye N,N'-dipentyl-3,4,9,10-perylenedicarboximide (pPDI) was obtained from Sigma-Aldrich and diluted to  $5 \times 10^{-9}$  M in toluene. The dye BODIPY268 was synthesized, as previously described by Paeng et al., and diluted in toluene to  $5 \times 10^{-9}$  M.<sup>24</sup> Molecular structure of the dyes is shown in Fig. S1. These solutions were then further diluted in the polystyrene solutions and spin-coated at 2000-3000 rpm onto a silicon wafer [≈6.5 × 6.5 mm<sup>2</sup>, cleaned with piranha solution (H<sub>2</sub>SO<sub>4</sub>:H<sub>2</sub>O<sub>2</sub> = 1:1)], resulting in films of at least 200 nm thickness as measured by ellipsometry. We note that dynamics in films of such thickness are expected to be dominated by bulk dynamics, as has been demonstrated by a variety of approaches including single molecule measurements;<sup>25-27</sup> even if some probes do display dynamics influenced by the free or supported surface, such probe molecules are unlikely to be detected in our study for multiple reasons, including their relative rarity in the sample and the expected large differences in dynamics between the surface and bulk molecules that would result in such molecules being outside the dynamic range of the measurement. The fluorophore concentrations in the final sample provided on average 200 analyzable fluorophores per field of view while simultaneously avoiding the presence of more than one probe molecule within a diffraction limited spot. Prior to single molecule measurements, each sample was placed in a vacuum cryostat (Janis ST-500) integrated with a homebuilt wide-field microscope and held at ~1.8 mTorr. The vacuum cryostat provides temperature control, facilitates removal of toluene from the sample, and limits oxygen-induced photobleaching of the fluorescent probes. Once the sample was placed in the cryostat, the temperature was raised to a minimum of 10 K above the glass transition temperature, as reported by Polymer Source, and held there for at least 1 h to assist in the removal of residual solvent, ensure stable pressure, and allow chain relaxation following spin-coating.  $^{28}$  In all but the lowest molecular weight system, this temperature was above the boiling point of the solvent (110–111  $^{\circ}$ C). In contrast, to remove residual solvent in the lowest molecular weight samples, the samples were held under vacuum for a minimum of 16 h. After solvent removal, all samples were lowered to the data collection temperature and held there for several hours to ensure the system was thermally equilibrated.

## **Imaging**

A continuous wave diode Nd:Vanadate laser (532 nm) was coupled into a multimode fiber (Newport, F-MCB-T-1FC) that was shaken at constant frequency and amplitude by a speaker to eliminate speckles and produce a randomly polarized and homogeneously illuminated field of view (diameter  $\approx 100 \, \mu \text{m}$ ). The light was focused at the back of the objective lens (Zeiss, LD Plan-Neofluar, air  $63\times$ , NA = 0.75) and into the cryostat to illuminate the sample. Fluorescence was collected in the epi-direction, through the same objective lens, and then passed through a dichroic mirror and long-pass (Semrock, LP03-532RU-25) and bandpass (Semrock, FF01-582/75) filters. A Wollaston prism was used to split the image into orthogonal polarizations which were imaged onto an electron multiplying charge-coupled device camera (EMCCD; Andor iXon DV887). Excitation power ranged from 10 to 15 mW at the back of the objective lens corresponding to a power density of 100-150 W/cm<sup>2</sup> at the sample. Most movies were taken at a temperature that resulted in a median relaxation time  $(\tau_{fit})$  of  $\approx 4$  s. To best capture rotational dynamics of a majority of molecules, a frame rate of 5 Hz was chosen (exposure time of 0.2 s) for these movies, which corresponds to ≈20 frames per median relaxation time. Additional movies were taken to confirm the predicted temperature dependences. These movies were taken at various frame rates, ranging from 0.14 to 125 Hz. For frame rates at and above 5 Hz, movies were collected continuously, while movies with lower frame rates were collected with a 0.2 s exposure time with illumination shuttered between frames to limit photobleaching. For each molecular weight, several long movies were collected at different locations in the same sample such that data were collected from at least 1000 molecules for each host and probe combination. All temperatures were corrected to account for a small degree of sample heating (typically 0.6 K) using an approach described previously.<sup>2</sup>

## Data analysis

All analysis was performed using the Interactive Data Language (IDL) software package, as described in detail in Hoang et al. <sup>29</sup> Briefly, molecules were chosen from a bandpassed set of 500 summed images found in the temporal middle of the longest movies. Subsequent analysis was performed on the raw and unfiltered images. Polarized fluorescence intensities ( $I_s$ ,  $I_p$ ) of the selected molecules were extracted from the two orthogonal polarization images of each molecule collected on the CCD at each timepoint. Single molecule linear dichroism (LD) was then calculated via LD(t) = ( $I_s - I_p$ )/( $I_s + I_p$ ), and an autocorrelation function was constructed using  $C(t) = \sum_{t'} a(t') \cdot a(t'+t)$ ]/[ $\sum_{t'} a(t') \cdot a(t')$ ], where a(t) = LD(t) -  $\langle$ LD(t) $\rangle$ . Least-squares fitting was used to fit each

autocorrelation function to the KWW function (C(t) = C(0)) $\exp[-(t/\tau_{fit})^{\beta}]$ ). For analysis of full-length movies, the correlation function was fit until it decayed to 0.1. C(t) values were constrained to  $0.2 < \beta < 2.0$  and 0.3 < C(0) < 2.0, and the average rotational correlation time,  $\tau_c$ , was calculated from the fit values of  $\tau_{fit}$  and  $\beta$  via  $\tau_c = (\tau_{fit}/\beta) \cdot \Gamma(1/\beta)$ , where  $\Gamma$  is the gamma function. Due to the lower signal to noise in movies collected with BODIPY268 as the probe, C(0) constraints were lifted for movies taken with this dye. Following analysis of the full-length movies, the movies were cut to a specified number of frames to allow analysis of single molecule dynamics as a function of trajectory length. C(0) and  $\beta$ constraints were lifted for this trajectory-dependent analysis, and the only constraint remaining was (number of frames)/ $\tau_{fit} \geq 2$ . Quasi-ensemble autocorrelations (ACFQE) were constructed by averaging autocorrelation functions from individual movies and then further weight averaged across movies for a particular probe and polystyrene molecular weight based on the number of molecules per movie.  $\beta_{QE}$  was then obtained by fitting the ACF<sub>QE</sub> to the KWW form.

### Inverse Laplace transform (ILT) distributions

An in-depth discussion on constructing ILT distributions is given in Ref. 24. In brief, the ILT of a stretched exponential function can be expressed by

$$\exp\left[-\left(t/\tau_{fit}\right)^{\beta}\right] = \int_{-\infty}^{\infty} P(\log \tau; \tau_{fit}, \beta) \cdot \exp\left(-t/\tau_{fit}\right) d\log \tau,$$

which assumes that a stretched exponential form results from a superposition of exponential relaxations with different relaxation times. The distribution of the normalized probability density function,  $P(log\,\tau;\,\tau_{fit},\,\beta),$  can be numerically obtained for any  $\tau_{fit}$  and  $\beta$ values and reflects the distribution of exponential relaxations that constitute the stretched exponential function. The ILT is first performed on the ACF<sub>OE</sub>, giving rise to a distribution we term the ILT distribution. This distribution is compared to a summed distribution of ILTs associated with each single molecule autocorrelation function. To construct this distribution, a set of reference distributions for  $\tau_{fit} = 1$  and  $\beta$  ranging from 0.20 to 0.99 in 0.01 steps was built previously. These reference distributions were used to approximate the distribution for any  $\tau_{fit}$  and  $\beta$  values obtained experimentally and were then shifted in  $\tau$  to match the measured  $\tau_{fit}$ . For any given single molecule data set, the single molecule ILT distributions were averaged and normalized by the area under the distribution to produce a distribution we term the ILT-built distribution.

#### **RESULTS AND DISCUSSION**

Previous studies have shown that the glass transition temperatures of polystyrene and other polymers vary with molecular weight and plateau at long chain length.<sup>2,5,30,31</sup> Dalle-Ferrier *et al.* have suggested that for rigid polymers such as polystyrene, this saturation will occur between 30 and 100 kg mol<sup>-1</sup>, consistent with the measurements of Ding *et al.*<sup>10,32</sup> Here, we study the dynamics of polystyrene ranging from 0.6 to 1364 kg mol<sup>-1</sup>, with a particular focus on lower molecular weights, to capture changes that

can be detected by single molecule rotational measurements that may exist as a function of molecular weight, glass transition temperature, and fragility. In two previous reports, we showed that the fluorescent probe pPDI demonstrates dynamics slaved to moderate molecular weight (168 kg mol $^{-1}$ ) polystyrene and reports that polystyrene displays significant dynamic heterogeneity over temperatures from 1.00 to 1.02  $T_g$  (373.0–383.6 K), yielding both median single molecule ( $\beta_{med}$ ) and quasi-ensemble ( $\beta_{QE}$ ) stretching exponents of  $\approx\!0.50$ , similar to those reported by bulk probe-free experiments.  $^{6.19,33,34}$ 

In the current study, first, we experimentally identified temperatures that yielded the desired rotational dynamics in polystyrene of each molecular weight with a target of  $\tau_{fit}=4~s.$  Rotations on this time scale can be captured straightforwardly with the CCD set to a frame rate of 5 Hz and with a dynamic range of at least 1 decade to each side of the median relaxation time. The temperatures identified in this manner track measured values of  $T_g$  as a function of molecular weight, as reported by Hintermeyer  $et~al.^{31}$  We also note that these temperatures track measured values of fragility as a function of polystyrene molecular weight [Fig. 1(a)].  $^{32}$  All data were initially collected at long trajectory lengths (or observation times) corresponding to  $\approx\!900~\tau_{fit}$ , a length previously recognized to allow the probes to explore all dynamic environments as reflected in a median  $\beta$  value that does not evolve further with longer observation time.  $^{19,34}$ 

Additional experiments were then undertaken to confirm that pPDI in both high and low molecular weight polystyrene yielded expected temperature dependences [Fig. 1(b)]. As we reported previously, in 168 kg mol<sup>-1</sup> polystyrene, the temperature dependence of probe rotational correlation times follows that reported by Roland et al.<sup>6,34</sup> In the 0.6 kg mol<sup>-1</sup> polystyrene, a less pronounced temperature dependence is apparent, consistent with the expected lower fragility of this lower molecular weight polystyrene. Fragility, m, can be defined as  $m = \frac{d \log(\tau_{\alpha})}{d(T_{g}/T)}\Big|_{T_{g}}$ , and fragility values reported here were calculated from the tangent of the best fits of log( $\tau_c$ ) vs  $T_g/T$ data at T<sub>g</sub>. This yields fragilities of ≈75 for the lowest molecular weight (0.6 kg mol<sup>-1</sup>) and 120 for the higher (168 kg mol<sup>-1</sup>) molecular weight polystyrene. This matches trends found in the literature, reinforcing that pPDI is an appropriate probe for characterizing polystyrene across molecular weights, even for systems where T<sub>g</sub> varies by more than 100 K. 10,31,32,3

From the same measurements that yield the  $\tau_c$  values shown in Fig. 1(b), the full distribution of time scales reported by the single molecules is also available. Figure 2(a) shows the distributions of  $\tau_{\rm fit}$  values for all pPDI probes measured in polystyrene across molecular weights, each at the temperature that led to median  $\tau_{\rm fit}\approx 4$  s. No difference in the breadth of relaxation times, as reflected by  $\tau_{\rm fit}$  values across molecular weights probed, is apparent. The distribution of  $\beta$  values does, however, shift to higher values for the lowest molecular weight polystyrene [Fig. 2(b)], suggesting that the lowest molecular weight polystyrene is less dynamically heterogeneous than the others.

To further examine dynamic heterogeneity, and in particular time scales associated with a dynamic exchange as a function of molecular weight in polystyrene,  $\tau_{\rm fit}$  and  $\beta$  distributions were evaluated as a function of trajectory length, with the premise that observing individual molecules for short times reveals time-local dynamics

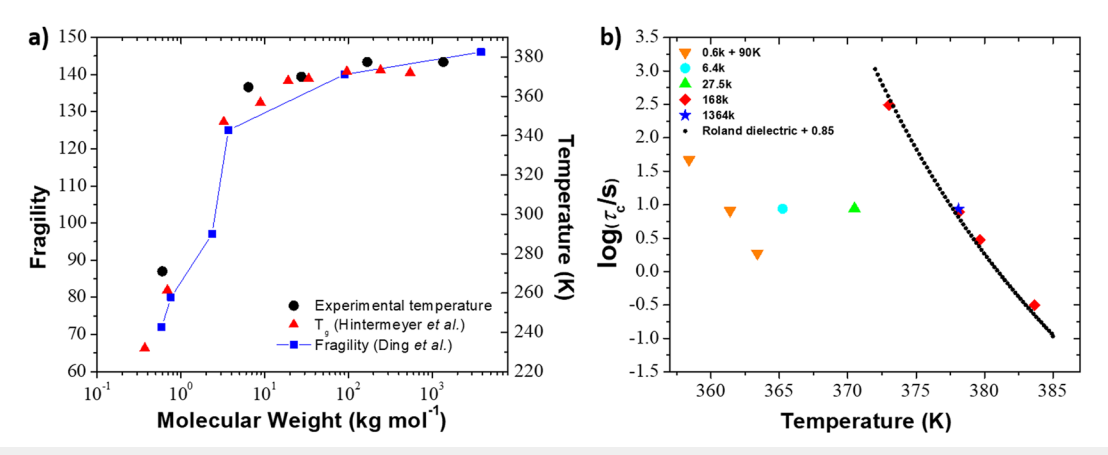


**FIG. 1.** (a) Fragility (blue squares, left axis) adapted from Ding *et al.*<sup>32</sup> compared to temperatures at which dynamics were captured in the current report (black circles, right axis) as well as  $T_g$  values from Hintermeyer *et al.*<sup>31</sup> (red triangles, right axis), each as a function of polystyrene molecular weight. (b) Measured median  $\tau_c$  values of pPDI as a function of temperature and polystyrene molecular weight. Measurements in 0.6 kg mol<sup>-1</sup> polystyrene are plotted 90 K higher than the actual measured temperature. Data collected in 168 kg mol<sup>-1</sup> polystyrene are compared to the Vogel-Fulcher-Tamman (VFT) fit of the temperature dependence reported by Roland and co-workers from dielectric spectroscopy measurements and shifted by 0.85 decades.<sup>6</sup>

experienced by the molecule, while observing molecules for long times allows them to experience and report changes in dynamics.  $^{24,36}$  For the full set of single molecules investigated, it is thus expected that the widths of the  $\tau_{\rm fit}$  and  $\beta$  distributions will decrease and median  $\beta$  values will decrease with increased observation time or trajectory length. This approach was previously used to characterize exchange time,  $\tau_{ex}$ , as a function of temperature in 168 kg mol $^{-1}$  polystyrene using pPDI as a probe and revealed no difference in overall degree of dynamic heterogeneity (as reported by  $\beta$ ) or exchange time relative to structural relaxation time  $(\tau_{ex}/\tau_{\alpha})$  as a function of temperature.  $^{19}$  For this analysis, the single molecule trajectories associated with the data shown in Fig. 2 were cut to shorter lengths ranging from  $\approx 30$  to 500  $\tau_{\rm fit}$  and refit to obtain new KWW

parameters and distributions that were then analyzed as a function of trajectory length (Fig. 3). While some variation in  $\tau_{fit}$  distribution width as a function of trajectory length for different molecular weight polystyrene is apparent [Fig. 3(a)], no clear trend as a function of molecular weight is observed. Additionally, no differences are seen in the width of the  $\beta$  distributions vs trajectory length as a function of molecular weight [Fig. 3(a), inset]. This is expected given that this quantity has been shown to be dominated by finite trajectory length effects rather than host dynamic heterogeneity.  $^{36,37}$  Evolution of the median  $\beta$  value as a function of trajectory length was also investigated [Fig. 3(b)]. At short trajectory lengths, the evolution of the median  $\beta$  value is very similar for all molecular weights. However, starting at trajectories of  $\approx 200~\tau_{fit}$  in length, the

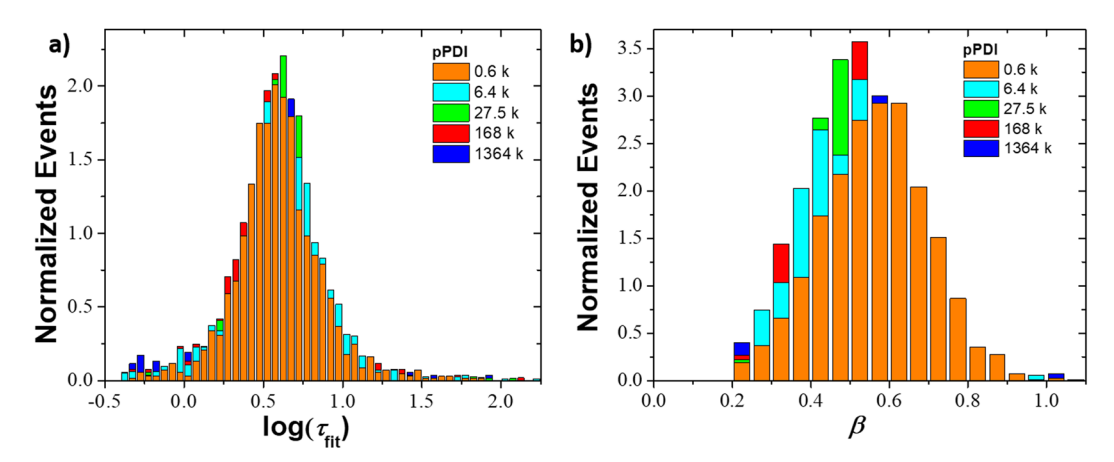


FIG. 2. (a)  $\tau_{fit}$  and (b)  $\beta$  distributions of pPDI in all molecular weights of polystyrene for the longest trajectory length measurements. While no change in  $\tau_{fit}$  distribution is observed, the  $\beta$  distribution shifts to higher values for the lowest molecular weight polystyrene. All distributions are shown separately in Fig. S2, and detailed distribution characteristics are given in Table S1 of the supplementary material.

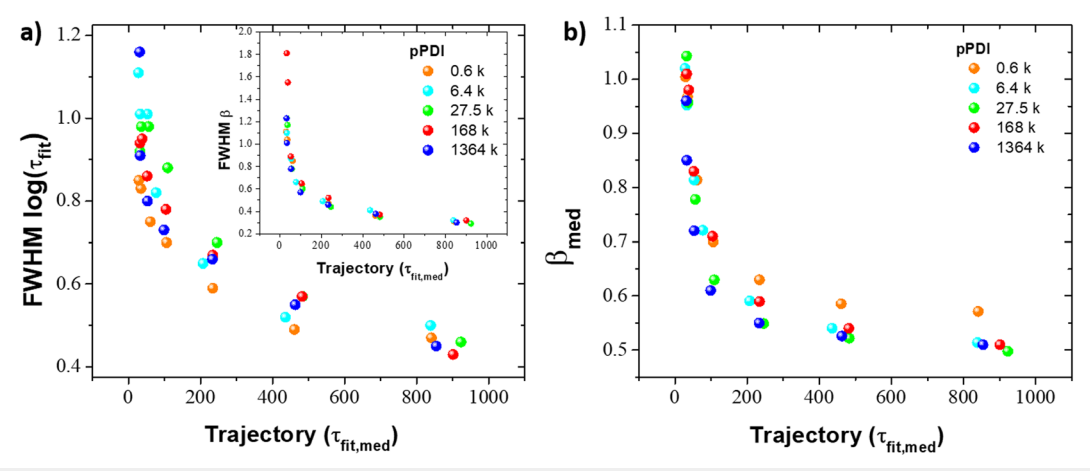


FIG. 3. The evolution of (a) the FWHM of  $log(\tau_{fit})$  and (inset)  $\beta$  and (b) median  $\beta$  with trajectory length of the pPDI in polystyrene data also shown in Fig. 2.

lowest molecular weight polystyrene shows consistently higher median  $\beta$  values than the other molecular weights, consistent with the distinctly right-shifted  $\beta$  distribution seen in Fig. 2(b), with the plateau median  $\beta$  value of  $\approx\!0.57$ , suggesting a lesser degree of dynamic heterogeneity compared to the higher molecular weight polystyrenes, where the  $\beta$  values plateau to  $\approx\!0.50$ . The evolution of the  $\beta$  value to a plateau occurs on similar time scales for all molecular weights, suggesting that the time scale of dynamic exchange does not vary with molecular weight or fragility in this system (Fig. 3). This was further reinforced by an analysis also used in Ref. 34 in which molecules from the initial fastest, middle, and slowest quintile were followed as a function of trajectory length (Fig. S3). No systematic difference in the time scale required for the fast or slow molecules to become average was seen as a function of polystyrene molecular weight.

Given the differences in measured and reported fragility over the polystyrene molecular weight range investigated here and the very large change in glass transition temperature over this range, the relatively modest differences seen in measured single molecule β values and time scales associated with dynamic exchange across the systems studied were somewhat surprising. In particular, the  $\beta$  value for low molecular weight polystyrene plateaued at  $\approx 0.57$ , whereas all higher molecular weight hosts plateaued at  $\beta \approx 0.50$ even while previous measurements had shown differences in fragility across most of the molecular weight range explored. Additionally, while  $\beta \approx 0.50$  is in the range of previous reports, it is higher than some reported values of probe-free or small probe ensemble or subensemble measurements of  $\beta$  in moderate to high molecular weight polystyrene near Tg. 6,2 <sup>5,38,39</sup> For example, Ediger and co-workers reported a β value as low as 0.35 using a fluorescence recovery after photobleaching approach with the probe tetracene in 50 kg mol<sup>-1</sup> polystyrene (expected fragility > 100) and Plazek et al. reported  $\beta \approx 0.35$  for polystyrene with a fragility of 139 in probefree experiments.<sup>38,39</sup> Taken together, these findings hinted that the pPDI probe may actually not report the full breadth of heterogeneity present in moderate to high molecular weight polystyrene, instead averaging over some dynamic heterogeneity in the system. This is plausible given that the probe rotational correlation time is  $\approx 7$  times slower than the high-molecular weight host segmental dynamics ( $\tau_c/\tau_\alpha=7.07$ ), and any difference in probe relative to host dynamics can result in probe averaging over dynamic environments in the host.  $^{40}$ 

Previously, a small BODIPY probe (BODIPY268) was used to characterize the molecular glass former o-terphenyl, with a  $\tau_c$  value nearly identical to that of the host, eliminating potential time averaging by the probe.<sup>24</sup> While BODIPY268 does not have the total photon yield of pPDI, limiting the signal to noise and/or trajectory length of measurements, it is approximately half the molecular weight of pPDI while exhibiting similar absorption and emission properties. It is thus a candidate to clarify whether pPDI reports of median  $\beta$  as a function of polystyrene molecular weight were impacted by potential averaging over dynamic heterogeneity in high fragility polystyrene. Because BODIPY268 has less favorable photophysics than pPDI, measurements are challenging and measurements were taken only in the 6.4 and 168.0 kg mol<sup>-1</sup> polystyrene samples, each at a single temperature. Again, temperature was adjusted to target a mean  $\tau_{fit}$  value of 4 s. For BODIPY268 measurements, this resulted in measurements at 364.3 and 374.8 K (Fig. S1). To estimate  $\tau_c/\tau_\alpha$  for BODIPY268 in polystyrene, using the VFT fit from Roland et al., the  $\tau_c$  value of pPDI in 168 kg mol<sup>-1</sup> polystyrene at 374.8 K was found and compared to that obtained via BODIPY268 measurements at the same temperature. This procedure suggested a  $\tau_c/\tau_\alpha$  value of  $\approx 1$  for BODIPY268 in polystyrene. We note that single molecule measurements of BODIPY268 in the lowest molecular weight polystyrene (0.6 kg mol<sup>-1</sup>) were not successful, possibly due to the combination of low probe signal and comparatively high host background, the latter of which most likely results from the lack of recrystallization of this low molecular weight polystyrene (for additional details, see Materials and Methods).

It is apparent from Fig. 4 that the  $\tau_{fit}$  and  $\beta$  distributions reported by BODIPY268 differ from those reported by pPDI for these (nearly) isochronic (same relaxation time) probe measurements. Notably, the median  $\beta$  values for the two molecular weights

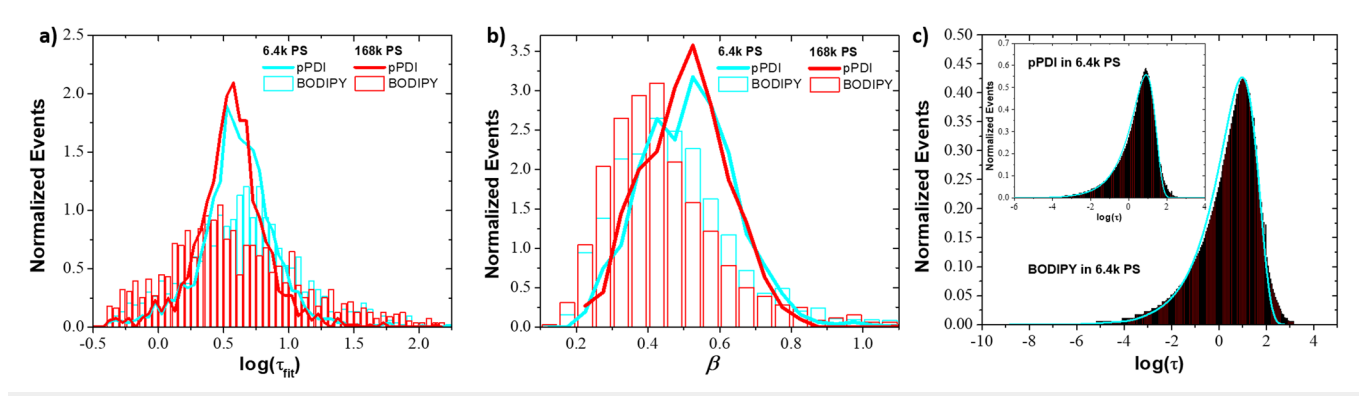
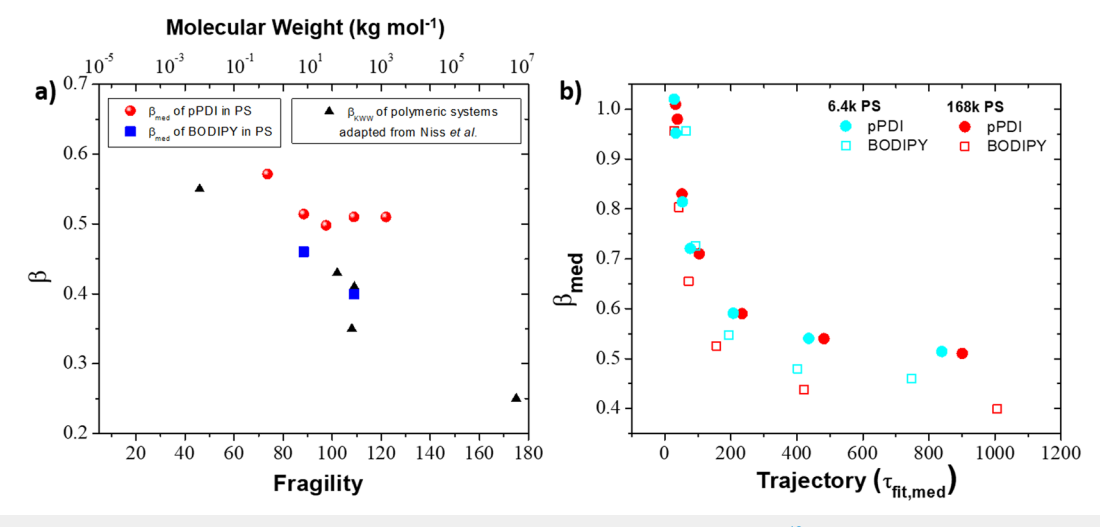


FIG. 4. (a) FWHM of  $\log(\tau_{\text{fit}})$  of polystyrene of two molecular weights using BODIPY268 (columns) overlaid by distributions for pPDI (lines) in polystyrene of the same molecular weights and similar trajectory lengths, with the pPDI data also shown in Fig. 2(a). (b)  $\beta$  distributions of the same systems shown in (a). Distributions of the BODIPY268 data are shown separately in Fig. S4, and detailed characteristics of this data are given in Table S2 of the supplementary material. (c) ILT-built distributions (columns) of 6.4 kg mol<sup>-1</sup> polystyrene as measured through BODIPY268 and (inset) pPDI and compared to that predicted from the ILT transform of the ACFsQE (lines). Equivalent distributions for 168 kg mol<sup>-1</sup> polystyrene are provided in Fig. S5 in the supplementary material.

measured are lower than those obtained from pPDI, with a value of  $\beta=0.46$  for the 6.4 kg  $mol^{-1}$  and  $\beta=0.41$  for the 168 kg  $mol^{-1}$ , suggestive of the fact that pPDI—despite capturing significant heterogeneity in moderate and high molecular weight polystyrene—may not capture its full dynamic heterogeneity. Given that BODIPY268 measurements are both noisier and yield shorter trajectories than pPDI in polystyrene, we checked consistency between single molecule reports and ensemble reports of heterogeneity for both probes. In this approach, described in more detail in Ref. 24, each individual single molecule autocorrelation is transformed through an inverse Laplace transform to yield the set of time scales experienced by each single molecule over the course of

the experiment. Such distributions are aggregated over all molecules as described in Materials and Methods. Assuming the single molecule traces offer robust reports of the dynamic environments probes experience, this approach should reproduce the distribution obtained from the inverse Laplace transform of the quasi-ensemble stretched exponential. For both pPDI and BODIPY268, the single molecule results match that obtained from the quasi-ensemble stretched exponential [Fig. 4(c) and Fig. S5], suggesting that the limitations associated with the BODIPY268 probe (in particular, relatively low signal to noise) do not preclude robust reporting of the local environments in polystyrene through single molecule measurements.



**FIG. 5.** (a)  $\beta$  values of various polymers as a function of isobaric fragility (black triangles), adapted from Niss *et al.*, <sup>13</sup> compared to measured median  $\beta$  values using pPDI (red circles) and BODIPY268 (blue squares) probes as a function of molecular weight. (b) The evolution of median  $\beta$  values of two moderate to high molecular weights of polystyrene using pPDI and BODIPY268. pPDI data are also shown in Fig. 3(b).

To more fully understand pPDI and BODIPY268 single molecule reports of polystyrene dynamic heterogeneity as a function of fragility, we compare median β values measured in this study to previous measurements. Examining isobaric fragility and stretching exponents compiled by Niss et al. for a variety of polymers [Fig. 5(a)], we find that measured  $\beta$  values, as reported by pPDI probes, do not follow the expected trends in mid to high molecular weight polystyrene, plateauing after the second lowest molecular weight polystyrene. We note that while the absolute value of fragility is path dependent, the general trend and thus correlation with molecular weight and stretching exponent are the same, regardless of path.<sup>13</sup> Furthermore, when comparing the fragility values of the molecular weights measured in the experiment of Ding et al. [Fig. 1(b)] to the predicted stretching exponents of Niss et al., the experimental β values obtained with pPDI do not agree with expectations. 13,32 This is consistent with the idea that pPDI averages over some dynamic heterogeneity in high fragility polystyrene. In contrast, the values obtained from BODIPY268 track closely with expectations suggested by Niss *et al.* [Fig. 5(a)].

Given this convergence between BODIPY268 results and previous measurements together with the fact that the pPDI probes did not reveal signs of variation in  $\tau_{ex}/\tau_{\alpha}$  as a function of fragility (Fig. 3), we performed trajectory length analysis for BODIPY268 probe measurements [Fig. 5(b)]. This analysis shows that even at relatively short trajectories, divergence between pPDI and BODIPY268  $\beta$  values are evident. Moreover, distinction between BODIPY268 results in the polystyrene of these two molecular weights is evident, not only at long trajectory lengths but also at shorter trajectory lengths, in contrast to findings in pPDI and consistent with the idea that BODIPY268 is more sensitive to differences in fragility than is pPDI. In accordance with previous work, we also

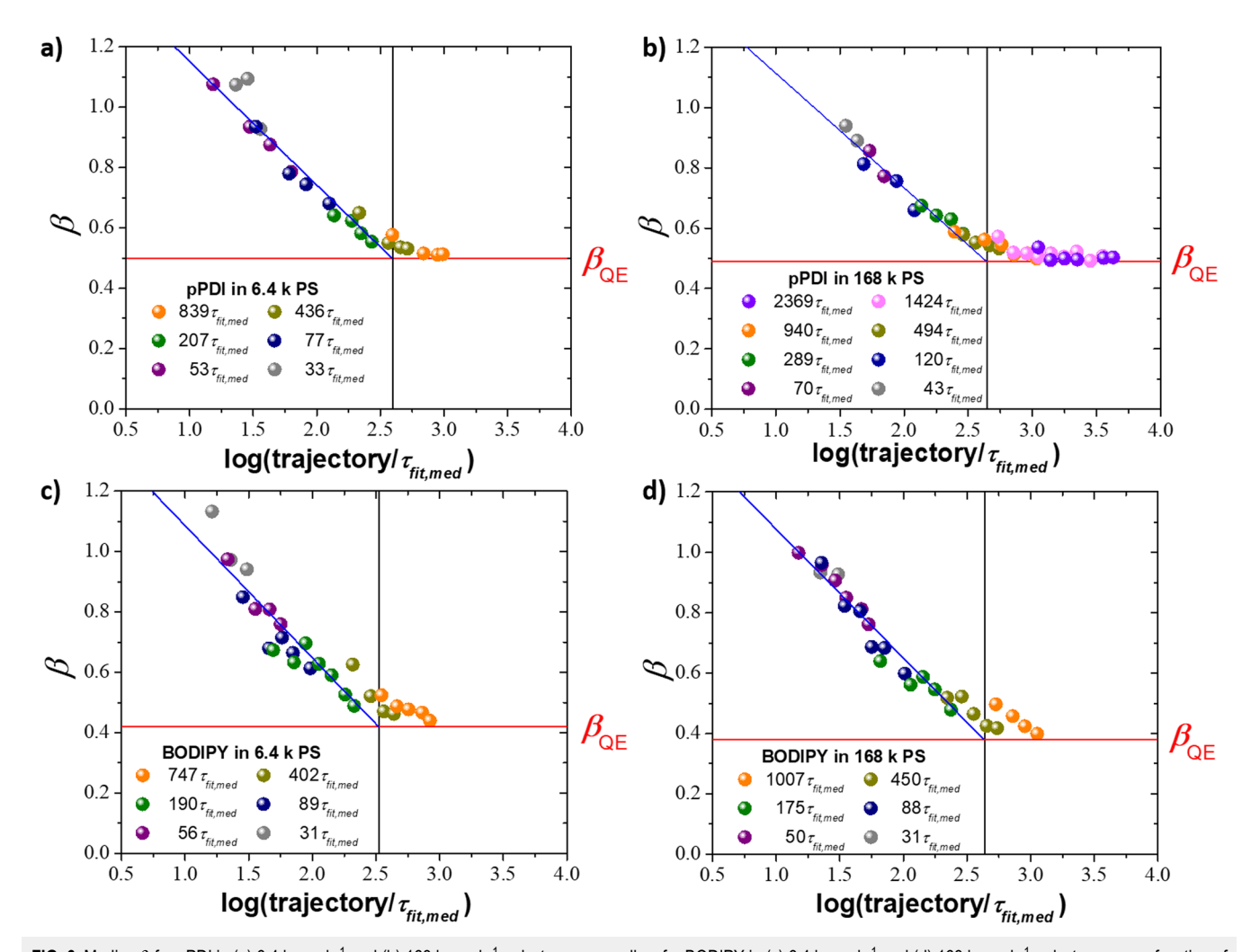


**FIG. 6.** Median  $\beta$  for pPDI in (a) 6.4 kg mol<sup>-1</sup> and (b) 168 kg mol<sup>-1</sup> polystyrene as well as for BODIPY in (c) 6.4 kg mol<sup>-1</sup> and (d) 168 kg mol<sup>-1</sup> polystyrene as a function of trajectory length for subsets of data of particular trajectory lengths. Data shown in (b) are also presented in Ref. 34. Characteristics of fits are given in Table S3, and vertical lines are drawn at the crossover times.

performed analysis of the evolution of median  $\beta$  using a procedure in which subsets of a given trajectory length were analyzed (Fig. 6). In brief, individual molecules of a given molecular weight and median trajectory length were grouped based on their individual  $\tau_{fit}$  values and trajectory lengths in terms of those individual  $\tau_{fit}$  values, and median  $\beta$  of each subset was plotted as a function of trajectory length. In all cases, the median  $\beta$  value decays with increasing trajectory length, reaching a plateau at the quasi-ensemble  $\beta$  value. In two previous papers, we showed that analyzing this decay can be used to characterize relative  $\tau_{ex}/\tau_{\alpha}$  values across variables such as temperature.  $^{19,34}$ 

Here, we use a related approach to characterize  $\tau_{ex}/\tau_{\alpha}$  as a function of polystyrene fragility as reported by pPDI and BODIPY268, fitting the linear portion of the descent of median  $\beta$  as a function of trajectory length to its plateau value, with the time of plateau characterizing the time scale on which the median probe molecule has explored all the dynamic environments available to it. This analysis reveals that the slopes of decay are similar for all probes (Table S3). Moreover, the time at which the single molecule median  $\beta$  value reaches the quasi-ensemble  $\beta$  value, which we term the crossover time, is quite similar in trajectory length in terms of probe rotations (Fig. 6, Fig. S6, and Table S3), with a shift to slightly higher values with increasing polystyrene fragility. The similarity in the decay rate and crossover times for median  $\beta$  values between the pPDI and BODIPY268 probes indicates that regardless of the degree of heterogeneity reported by the probe, the probe reports no further changes after a given number of probe rotations. This indicates that the difference in probe reports of dynamic heterogeneity in these systems is not due to missing dynamics on the long time side, consistent with our understanding of how probes may average over dynamic heterogeneity. 40 Additionally, the fact that crossover time varies little with host fragility indicates that while fragility and  $\beta$  are correlated and both likely intrinsic reporters of dynamic heterogeneity, time scales associated with dynamic exchange do not show strong correlation with either quantity.

### CONCLUSION

The dynamics of polystyrene of varied molecular weight were investigated via single molecule rotational measurements. Previous reports had shown that the fragility of polystyrene increases with molecular weight, and other studies had suggested a correlation between fragility and degree of dynamic heterogeneity, as reported by the stretching exponent,  $\beta$ . The current measurements revealed that single molecule reports of stretching exponents indeed decrease with increasing polystyrene molecular weight. While the fluorescent probe pPDI reported differences in  $\beta$  between very low molecular weight polystyrene and polystyrene of higher molecular weight, it did not differentiate between polystyrene systems with high fragilities. The smaller fluorescent probe, BODIPY268, uncovered a wider range of stretching exponents than pPDI, reinforcing the anticorrelation between  $\beta$  and fragility on the single molecule level across the full range of accessible fragilities. Despite this, neither probe showed strong evidence for correlation between characteristic time scales of dynamic exchange and β or fragility, suggesting no or limited inherent correlation between time scales of exchange and quantities that characterize the degree of glassy or anomalous behavior.

#### SUPPLEMENTARY MATERIAL

Additional details on the pPDI and BODIPY268 data are presented in six figures and three tables in the supplementary material.

#### **ACKNOWLEDGMENTS**

This work was supported by NSF Grant Nos. DGE 16-44869 and CHE 1660392. We thank Keewook Paeng for helpful discussions and assistance in collection of pPDI in 168 kg mol<sup>-1</sup> polystyrene data.

### **REFERENCES**

- <sup>1</sup>T. G. Fox and P. J. Flory, J. Am. Chem. Soc. **70**, 2384 (1948).
- <sup>2</sup>T. G. Fox and P. J. Flory, J. Appl. Phys. 21, 581 (1950).
- <sup>3</sup>T. G. Fox and P. J. Flory, J. Phys. Chem. 55, 221 (1951).
- <sup>4</sup>T. G. Fox and P. J. Flory, J. Polym. Sci. 14, 315 (1954).
- <sup>5</sup>P. G. Santangelo and C. M. Roland, Macromolecules **31**, 4581 (1998).
- <sup>6</sup>C. M. Roland and R. Casalini, J. Chem. Phys. 119, 1838 (2003).
- <sup>7</sup>C. Dalle-Ferrier, K. Niss, A. P. Sokolov, B. Frick, J. Serrano, and C. Alba-Simionesco, Macromolecules **43**, 8977 (2010).
- <sup>8</sup>C. A. Angell, Science **267**, 1924 (1995).
- <sup>9</sup>Q. Qin and G. B. McKenna, J. Non-Cryst. Solids **352**, 2977 (2006).
- <sup>10</sup>C. Dalle-Ferrier, A. Kisliuk, L. Hong, G. Carini, G. Carini, G. D'Angelo, C. Alba-Simionesco, V. N. Novikov, and A. P. Sokolov, J. Chem. Phys. **145**, 154901 (2016)
- <sup>11</sup>X. Xia and P. G. Wolynes, Proc. Natl. Acad. Sci. U. S. A. 97, 2990 (2000).
- <sup>12</sup> A. F. Kozmidis-Petrović, J. Therm. Anal. Calorim. 127, 1975 (2017).
- <sup>13</sup> K. Niss, C. Dalle-Ferrier, G. Tarjus, and C. Alba-Simionesco, J. Phys.: Condens. Matter 19, 076102 (2007).
- <sup>14</sup>D. M. Sussman, S. S. Schoenholz, E. D. Cubuk, and A. J. Liu, Proc. Natl. Acad. Sci. U. S. A. 114, 10601 (2017).
- <sup>15</sup>R. Richert, J. Phys.: Condens. Matter **14**, R703 (2002).
- <sup>16</sup>M. D. Ediger, Annu. Rev. Phys. Chem. **51**, 99 (2000).
- <sup>17</sup>R. Böhmer, K. L. Ngai, C. A. Angell, and D. J. Plazek, J. Chem. Phys. **99**, 4201 (1993).
- <sup>18</sup>G. Adam and J. H. Gibbs, J. Chem. Phys. **43**, 139 (1965).
- <sup>19</sup> A. S. Manz, K. Paeng, and L. J. Kaufman, J. Chem. Phys. **148**, 204508 (2018).
- <sup>20</sup>R. Böhmer, G. Hinze, G. Diezemann, B. Geil, and H. Sillescu, Europhys. Lett. **36**, 55 (1996).
- <sup>21</sup>C. Y. Wang and M. D. Ediger, J. Chem. Phys. 112, 6933 (2000).
- <sup>22</sup> A. N. Adhikari, N. A. Capurso, and D. Bingemann, J. Chem. Phys. **127**, 114508 (2007).
- <sup>23</sup> J. Qian and A. Heuer, Eur. Phys. J. B 18, 501 (2000).
- <sup>24</sup> K. Paeng, H. Park, D. T. Hoang, and L. J. Kaufman, Proc. Natl. Acad. Sci. U. S. A. 112, 4952 (2015).
- <sup>25</sup>R. Richert, Annu. Rev. Phys. Chem. **62**, 65 (2011).
- <sup>26</sup>K. Paeng, S. F. Swallen, and M. D. Ediger, J. Am. Chem. Soc. 133, 8444 (2011).
- <sup>27</sup>B. M. I. Flier, M. C. Baier, J. Huber, K. Müllen, S. Mecking, A. Zumbusch, and D. Wöll, J. Am. Chem. Soc. **134**, 480 (2012).
- <sup>28</sup> M. Tress, M. Erber, E. U. Mapesa, H. Huth, J. Müller, A. Serghei, C. Schick, K.-J. Eichhorn, B. Voit, and F. Kremer, Macromolecules 43, 9937 (2010).
- <sup>29</sup> D. T. Hoang, K. Paeng, H. Park, L. M. Leone, and L. J. Kaufman, Anal. Chem. 86, 9322 (2014).
- <sup>30</sup>V. N. Novikov and E. A. Rössler, *Polymer* **54**, 6987 (2013).
- <sup>31</sup> J. Hintermeyer, A. Herrmann, R. Kahlau, C. Goiceanu, and E. A. Rossler, Macromolecules 41, 9335 (2008).
- <sup>32</sup>Y. Ding, V. N. Novikov, A. P. Sokolov, A. Cailliaux, C. Dalle-Ferrier, C. Alba-Simionesco, and B. Frick, Macromolecules 37, 9264 (2004).

 <sup>&</sup>lt;sup>33</sup>C. T. Thurau and M. D. Ediger, J. Chem. Phys. **116**, 9089 (2002).
<sup>34</sup>K. Paeng and L. J. Kaufman, Macromolecules **49**, 2876 (2016).

<sup>&</sup>lt;sup>35</sup>C. G. Robertson, P. G. Santangelo, and C. M. Roland, J. Non-Cryst. Solids 275,

<sup>&</sup>lt;sup>36</sup>C. Y. Lu and D. A. Vanden Bout, J. Chem. Phys. **125**, 124701 (2006).

 <sup>&</sup>lt;sup>37</sup>K. Stokely, A. S. Manz, and L. J. Kaufman, J. Chem. Phys. **142**, 114504 (2015).
<sup>38</sup>T. Inoue, M. T. Cicerone, and M. D. Ediger, Macromolecules **28**, 3425

<sup>&</sup>lt;sup>39</sup>D. J. Plazek and K. L. Ngai, Macromolecules **24**, 1222 (1991).

<sup>&</sup>lt;sup>40</sup>K. Paeng and L. J. Kaufman, Chem. Soc. Rev. **43**, 977 (2014).